Geomechanics and Engineering, *Vol. 16, No. 2 (2018) 151-157*
DOI: https://doi.org/10.12989/gae.2018.16.2.151

Influence of interaction between coal and rock on the stability of strip coal pillar

W. Gao*

Key Laboratory of Ministry of Education for Geomechanics and Embankment Engineering, College of Civil and Transportation Engineering, Hohai University, Nanjing 210098, P. R. China

(Received June 27, 2017, Revised April 9, 2018, Accepted May 15, 2018)

Abstract. The constrained conditions of roof and floor for the coal pillar affect the strength of coal pillar very seriously. To analyze the influence of rock mass for the roof and floor on the stability of coal pillar comprehensively, one method based on the mechanical method for the composite rock mass was proposed. In this method, the three rock layers of roof, floor and coal pillar are taken as the bedded composite rock mass. And the influence of rock mass for the roof and floor on the elastic core of coal pillar has been analyzed. This method can obtain not only the derived stress by the cohesive constraining forces for the coal pillar, but also the derived stress for the rock mass of the roof and floor. Moreover, the effect of different mechanical parameters for the roof and floor on the stability of coal pillar have been analyzed systematically. This method can not only analyze the stability of strip coal pillar, but also analyze the stability of other mining pillars whose stress distribution is similar with that of the strip coal pillar.

Keywords: influence; strip coal pillar; stress distribution; derived stress; roof and floor

1. Introduction

One of the most important tasks to guarantee the safe mining of coal is to maintain the stability of coal pillars, especially for strip mining, room and pillar mining, etc. Therefore, there are enormous research studies underway on pillar stability, including the theoretical method (Gao 2014, Gao and Ge 2016, Jia *et al*. 2011, Li *et al*. 2011, Yang *et al*. 2015, Zhang JX *et al*. 2017), the numerical simulation method (Guo *et al*. 2016, Li *et al*. 2015, Shao and Xia 2011, Sherizadeh and Kulatilake 2016, Wang *et al*. 2016, Zhang GC *et al*. 2017, Zhang and Goh 2016, Zhang *et al*. 2013), and the engineering experience method (Chen SJ *et al*. 2016, Ghasemi *et al*. 2014, Mark 1999, Reed *et al*. 2017,Wattimena *et al*. 2013, Wilson 1972, Zhou *et al*. 2011). Those studies can provide theoretical equations or empirical formulae for the coal pillar width, the distribution of the stress and strain in the coal pillar and its surrounding rock mass, etc. Thus, the stability of coal pillars can be analysed. Although those studies can improve the principles of coal pillar design, they analyse only the stress and strength of coal pillars; the influence of the roof and floor on the coal pillar cannot be considered. Generally, the loading system of a coal pillar in a two-dimensional state is shown in Fig. 1(a). It is similar to the loading system for the test of uniaxial compressive rock strength, shown in Fig. 1(b).

Thus, the stress state of the coal pillar is similar to that of a rock specimen in the uniaxial compressive strength test. According to the basic theory of rock mechanics (Jaeger 2009), the strength of a rock specimen is affected seriously by the constrained conditions of its two ends. The constraints of the ends will increase the strength of the rock specimen. For the coal mine, the interaction of coal and rock affects their mechanical properties very seriously. Some researchers have studied on the interaction of coal and rock. For example, for one combined support system, the influence of interaction of coal and rock on the stability of deep coal roadways has been analysed by the numerical study (Chen M *et al*. 2016). The influence of interaction of coal and rock on the rock damage has been studied by the acoustic emission method and plastic strain theory (Jin *et al*. 2017). By using granular dynamic models, mechanical interactions of rock-coal composite samples has been studied (Zhang *et al*. 2018). Moreover, based on compressive simulation tests with 5 different interfacial angels of combined coal-rock samples conducted by PFC2D software, the influence of the interfacial angel on failure characteristics and mechanism of combined coal-rock mass has been studied (Zhao *et al*. 2016). Therefore, the constrained conditions of the roof and floor for the coal pillar should seriously affect the strength of the coal pillar. In other words, the stability of coal pillar will be affected by the mechanical properties of rock mass for roof and floor. There are some studies for the influence of interaction between coal and rock on the stability of coal pillar. For example, based on the field measurement, Reed *et al*. (2017) proposed that the interaction between coal pillar and the overburden stiffness should be considered in the coal pillar design. Based on experimental study, the influence of interaction between coal pillar and the overburden on the stability of pillar-roof system has been investigated (Zhou *et al*. 2018). Moreover, the influence of interaction between coal pillar and the overburden on the stability of multiple

*Corresponding author, Professor
E-mail: wgaowh@163.com

ISSN: 2005-307X (Print), 2092-6219 (Online)

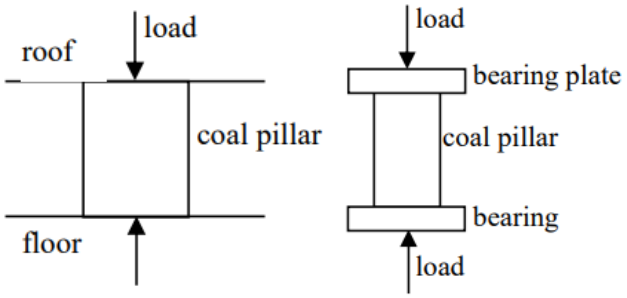

(a) Coal pillar system (b) Test system

Fig. 1 Loading system for the coal pillar and test of uniaxial compressive rock strength

pillars has been studied by numerical method (Zhou *et al*. 2017). However, the systematically mechanical analysis for the influence of rock mass for the roof and floor on the stability of coal pillar has not been studied in previous researches. Thus, in this study, based on the basic theories of rock mechanics and elastic mechanics (Sadd 2005), one method to analyze the influence of rock mass for the roof and floor on the stability of strip coal pillars is proposed. Moreover, through application in one real engineering example, the affections of the rock mass for the roof and floor on the stability of the strip coal pillar are researched.

2. Computational model and basic assumptions

Because the stability of a strip coal pillar is controlled by its confined elastic core (Gao 2014), in this study, the stability of the confined elastic core is analyzed.

To simplify the calculation and avoid significant errors, the follow assumptions are made:

a. The confined elastic core of the coal pillar is in the triaxial compression stress state, and its upper and lower strata are in this state, too (Guo and Cai 2008, Wu *et al*. 1994);

b. The cohesive forces between the confined elastic core and its upper and lower strata are large enough (Wu *et al*. 1994), thus they can be described as the bedded composite rock mass (Tan and Xian 1994).

Based on the above assumptions, the computational model for the confined elastic core of a coal pillar is shown in Fig. 2. In this model, the rock strata of the roof, the coal pillar, and the rock strata of the floor are indicated as rock layers *A*, *B* and *C*, respectively.

As typical rock layers of coal mine, for the coal stratum, rock strata of roof and floor, generally, there are following equations (Li and Lian 2011)

$$\begin{cases} E_A > E_B \\ E_C > E_B \end{cases} \tag{1}$$

$$\mu_A < \mu_B\,,\ \ \mu_C < \mu_B \tag{2}$$

where E_A, E_B and E_C are the elastic modulus for the three layers, and μ_A, μ_B and μ_C are the Poisson's ratios for the three layers.

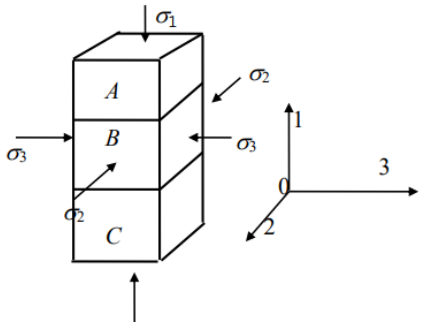

Fig. 2 Computational model of the coal pillar

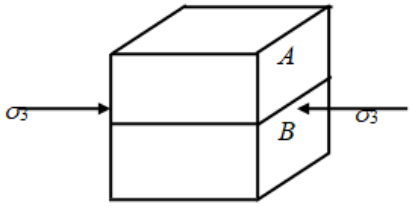

Fig. 3 Computational model of the interfacial unit between layers *A* and *B* by the compression of σ_3

3. Stress analysis of the interfacial unit between two layers

According to the stress superposition principle (Sadd 2005), the triaxial compression stress can be described by the superposition of three uniaxial compression stresses. Thus, the mechanical analysis of the interfacial unit between two layers is as follows.

3.1 Analysis of the interfacial unit between layers A and B

First, the stress-strain analysis of the interfacial unit by the stress of σ_3 is conducted. The computational model is shown in Fig. 3.

Because of E_A>E_B and $\mu_A < \mu_B$, the derived stress can be created in the interfacial unit by the cohesive constraining forces (Tan and Xian 1994). Generally, along orientation 2, the derived tensile stress can be created in layer *A*, and the derived compressive stress can be created in layer *B*. Moreover, along orientation 3, the derived compressive stress can be created in layer *A*, and the derived tensile stress can be created in layer *B* (Tan and Xian 1994). Based on the deformation continuity condition and static equilibrium condition (Li and Lian 2011), there are the following equations

$$\begin{cases} \varepsilon_{3A}^{3AB} = \varepsilon_{3B}^{3AB} \\ \varepsilon_{2A}^{3AB} = \varepsilon_{2B}^{3AB} \\ \sigma_{3A}^{3AB} = \sigma_3 + \sigma_3^{3AB} \\ \sigma_{3B}^{3AB} = \sigma_3 - \sigma_3^{3AB} \\ \sigma_{2A}^{3AB} = \sigma_{2B}^{3AB} = \sigma_2^{3AB} \\ \sigma_{1A}^{3AB} = \sigma_{1B}^{3AB} = 0 \end{cases} \tag{3}$$

where ε_{3A}^{3AB}, ε_{2A}^{3AB}, ε_{3B}^{3AB} and ε_{2B}^{3AB} are the strains in the layers *A* and *B* for the interfacial unit along the orientation 3 and 2, respectively. σ_{3A}^{3AB},σ_{3B}^{3AB}, σ_{2A}^{3AB}, σ_{2B}^{3AB}, σ_{1A}^{3AB} and σ_{1B}^{3AB} are the stresses in layers *A* and *B* for the interfacial unit along orientations 3, 2 and 1, respectively. σ_{3}^{3AB} and σ_{2}^{3AB} are the derived stresses in layers *A* and *B* for the interfacial unit along orientations 3 and 2, respectively. The orientations 3, 2 and 1 are shown in Fig. 2.

Combining the generalized Hooke law (Sadd 2005) which is as Eq. (4) and Eq. (3), Eq. (5) can be obtained.

$$\begin{cases} \varepsilon_{3A}^{3AB} = \dfrac{1}{E_A}[\sigma_{3A}^{3AB} - \mu_A(-\sigma_{2A}^{3AB})] \\ \varepsilon_{2A}^{3AB} = \dfrac{1}{E_A}(-\sigma_{2A}^{3AB} - \mu_A\sigma_{3A}^{3AB}) \\ \varepsilon_{3B}^{3AB} = \dfrac{1}{E_B}(\sigma_{3B}^{3AB} - \mu_B\sigma_{2B}^{3AB}) \\ \varepsilon_{2B}^{3AB} = \dfrac{1}{E_B}(\sigma_{2B}^{3AB} - \mu_B\sigma_{3B}^{3AB}) \end{cases} \tag{4}$$

$$\begin{cases} \sigma_{3A}^{3AB} = \sigma_3 + k_{1AB}\sigma_3 \\ \sigma_{3B}^{3AB} = \sigma_3 - k_{1AB}\sigma_3 \\ \sigma_{2A}^{3AB} = -k_{2AB}\sigma_3 \\ \sigma_{2B}^{3AB} = k_{2AB}\sigma_3 \\ \sigma_{1B}^{3AB} = \sigma_{1A}^{3AB} = 0 \end{cases} \tag{5}$$

where

$$k_{1AB} = \frac{E_A^2(1-\mu_B^2) - E_B^2(1-\mu_A^2)}{(E_A+E_B)^2 - (E_A\mu_B + E_B\mu_A)^2} \tag{6}$$

$$k_{2AB} = \frac{2E_AE_B(\mu_B - \mu_A)}{(E_A+E_B)^2 - (E_A\mu_B + E_B\mu_A)^2} \tag{7}$$

Second, the stress–strain analysis of the interfacial unit by the stress of σ_2 is conducted. Using the same method as above, there are the following equations,

$$\begin{cases} \sigma_{3A}^{2AB} = -k_{4AB}\sigma_2 \\ \sigma_{3B}^{2AB} = k_{4AB}\sigma_2 \\ \sigma_{2A}^{2AB} = \sigma_2 + k_{3AB}\sigma_2 \\ \sigma_{2B}^{2AB} = \sigma_2 - k_{3AB}\sigma_2 \\ \sigma_{1B}^{2AB} = \sigma_{1A}^{2AB} = 0 \end{cases} \tag{8}$$

where σ_{3A}^{2AB}, σ_{3B}^{2AB}, σ_{2A}^{2AB}, σ_{2B}^{2AB}, σ_{1A}^{2AB} and σ_{1B}^{2AB} are the stresses in layers *A* and *B* for the interfacial unit along orientations 3, 2 and 1, respectively. k_{3AB}=k_{1AB}. K_{4AB}=k_{2AB}.

Third, the stress–strain analysis of the interfacial unit by the stress of σ_2 is conducted. In this state, generally, along orientations 2 and 3, the derived tensile stress can be created in layer *A*, and the derived compressive stress can be created in layer *B*. Using the same method as above, there are the following equations

$$\begin{cases} \sigma_{3A}^{1AB} = \sigma_{2A}^{1AB} = -k_{5AB}\sigma_1 \\ \sigma_{3B}^{1AB} = \sigma_{2B}^{1AB} = k_{5AB}\sigma_1 \\ \sigma_{1B}^{1AB} = \sigma_{1A}^{1AB} = \sigma_1 \end{cases} \tag{9}$$

where

$$k_{5AB} = \frac{E_A^2(\mu_B^2+\mu_B) - E_B^2(\mu_A^2+\mu_A) + E_AE_B(\mu_B-\mu_A)}{(E_A+E_B)^2 - (E_A\mu_B + E_B\mu_A)^2} \tag{10}$$

σ_{3A}^{1AB}, σ_{3B}^{1AB}, σ_{2A}^{1AB}, σ_{2B}^{1AB}, σ_{1A}^{1AB} and σ_{1B}^{1AB} are the stresses in layers *A* and *B* for the interfacial unit along orientations 3, 2 and 1, respectively.

Finally, according to the stress superposition principle, the stresses in layers *A* and *B* for the interfacial unit under the triaxial compression state are

$$\begin{cases} \sigma_{3A}^{AB} = (\sigma_3 + k_{1AB}\sigma_3) - k_{2AB}\sigma_2 - k_{5AB}\sigma_1 \\ \sigma_{2A}^{AB} = -k_{2AB}\sigma_3 + \sigma_2 + k_{1AB}\sigma_2 - k_{5AB}\sigma_1 \\ \sigma_{1A}^{AB} = \sigma_1 \end{cases} \tag{11}$$

$$\begin{cases} \sigma_{3B}^{AB} = (\sigma_3 - k_{1AB}\sigma_3) + k_{2AB}\sigma_2 + k_{5AB}\sigma_1 \\ \sigma_{2B}^{AB} = k_{2AB}\sigma_3 + \sigma_2 - k_{1AB}\sigma_2 + k_{5AB}\sigma_1 \\ \sigma_{1B}^{AB} = \sigma_1 \end{cases} \tag{12}$$

where σ_{3A}^{AB}, σ_{3B}^{AB}, σ_{2A}^{AB}, σ_{2B}^{AB}, σ_{1A}^{AB} and σ_{1B}^{AB} are the stresses in layers *A* and *B* for the interfacial unit along orientations 3, 2 and 1, respectively.

3.2 Analysis of the interfacial unit between layers B and C

Using the same method as in section 3.1, the stresses in layers *B* and *C* for the interfacial unit under the triaxial compression state are

$$\begin{cases} \sigma_{3B}^{BC} = (\sigma_3 - k_{1BC}\sigma_3) + k_{2BC}\sigma_2 + k_{5BC}\sigma_1 \\ \sigma_{2B}^{BC} = k_{2BC}\sigma_3 + \sigma_2 - k_{1BC}\sigma_2 + k_{5BC}\sigma_1 \\ \sigma_{1B}^{BC} = \sigma_1 \end{cases} \tag{13}$$

$$\begin{cases} \sigma_{3C}^{BC} = (\sigma_3 + k_{1BC}\sigma_3) - k_{2BC}\sigma_2 - k_{5BC}\sigma_1 \\ \sigma_{2C}^{BC} = -k_{2BC}\sigma_3 + \sigma_2 + k_{1BC}\sigma_2 - k_{5BC}\sigma_1 \\ \sigma_{1C}^{BC} = \sigma_1 \end{cases} \tag{14}$$

where

$$k_{1BC} = \frac{E_C^2(1-\mu_B^2) - E_B^2(1-\mu_C^2)}{(E_C+E_B)^2 - (E_C\mu_B + E_B\mu_C)^2} \tag{15}$$

$$k_{2BC} = \frac{2E_CE_B(\mu_B - \mu_C)}{(E_C+E_B)^2 - (E_C\mu_B + E_B\mu_C)^2} \tag{16}$$

$$k_{5BC} = \frac{E_C^2(\mu_B^2+\mu_B) - E_B^2(\mu_A^2+\mu_A) + E_CE_B(\mu_B-\mu_C)}{(E_C+E_B)^2 - (E_C\mu_B + E_B\mu_C)^2} \tag{17}$$

It must be noted that the stress outside the interfacial area is not changed.

4. Strength analysis of the interfacial unit between two layers

In this study, the generally used Mohr-Coulomb strength criterion is applied (Jaeger 2009), which is,

$$\sigma_{1j} = k_p \sigma_{3j} + \sigma_c \tag{18}$$

where σ_{1j} and σ_{3j} are the maximum and minimum principal stresses, respectively, σ_c is the uniaxial compression strength, and K_p is a stress coefficient, which can be defined as follows

$$K_p = \frac{1+\sin\varphi}{1-\sin\varphi} \tag{19}$$

where φ is the effective internal friction angle.

According to the computation results in section 3.1, the maximum and minimum principal stresses of layers *A* and *B* in the interfacial area are

$$\begin{cases} \sigma_{1j}^{A} = \sigma_1 \\ \sigma_{3j}^{A} = \sigma_3(1+k_{1AB}) - k_{2AB}\sigma_2 - k_{5AB}\sigma_1 \end{cases} \tag{20}$$

$$\begin{cases} \sigma_{1j}^{B} = \sigma_1 \\ \sigma_{3j}^{B} = \sigma_3(1-k_{1AB}) + k_{2AB}\sigma_2 + k_{5AB}\sigma_1 \end{cases} \tag{21}$$

Eq. (20) is substituted into Eq. (18). The strength of the layer *A* in the interfacial area is

$$\sigma_{1jA} = \frac{k_{pA}[\sigma_3(1+k_{1AB}) - k_{2AB}\sigma_2] + \sigma_{cA}}{1 + k_{pA}k_{5AB}} \tag{22}$$

Using the same method, the strength of layer *B* in the interfacial area is

$$\sigma_{1jB} = \frac{k_{pB}[\sigma_3(1-k_{1AB}) + k_{2AB}\sigma_2] + \sigma_{cB}}{1 - k_{pB}k_{5AB}} \tag{23}$$

The same method is used to analyze the strength of layers *B* and *C* in their interfacial areas. The strength of layer *B* is

$$\sigma_{1jB} = \frac{k_{pB}[\sigma_3(1-k_{1BC}) + k_{2BC}\sigma_2] + \sigma_{cB}}{1 - k_{pB}k_{5BC}} \tag{24}$$

The strength of the layer *C* is

$$\sigma_{1jC} = \frac{k_{pC}[\sigma_3(1+k_{1BC}) - k_{2BC}\sigma_2] + \sigma_{cC}}{1 + k_{pC}k_{5BC}} \tag{25}$$

However, the strengths of rock mass *A*, *B* and *C* outside the interfacial area are not changed, and are their normal triaxial compressive strengths.

5. Stability analysis of strip coal pillar

Based on above analysis, for the interfacial constraint, the compressive strength of the rock layer in the interfacial area will be changed. And the strength rely on the elastic modulus and the Poisson's ratio for all rock layers. Because these parameters can affect the stress state of the rock layers, their confining pressure will be changed. According to the basic principle of rock mechanics (Jaeger 2009), the triaxial compressive strength of the rock is controlled by its confining pressure. As the confining pressure increases, the triaxial compressive strength will increase too. As for the coal measure strata, this kind of interfacial effect will increase the strength of the coal pillar in the interfacial area, and decrease the strength of rock strata for the roof and floor in the interfacial area. Because the length and width of the strip coal pillar are much bigger than its height, generally, the interfacial effect will affect the whole height. Therefore, the strength of the whole coal pillar will be increased. Because the stability of strip coal pillar is controlled by the strength of its elastic core, the interfacial effect will increase the stability of the strip coal pillar. From the Eqs. (22)-(25), the higher the hardness of the roof and floor are and the lower that of coal pillar is, the larger the interfacial effect on the coal pillar will be.

6. Engineering example and discussion

To verify the method proposed in this study, one strip coal mining area in China is used (Gao and Ge 2016). This strip mining area is exploited by strip mining along the seam strike, whose elevation is between -495 and -600 m. The entire mining area is divided into four sections, which are four working faces, width of 25 m, and three strip coal pillars, width of 30 m. The height of coal pillar is 2.5 m. The rocks of the roof and floor for the coal seam are medium sandstone and grit sandstone. The mechanical parameters for the coal material and its surround rocks are summarized in Table 1.

Based on the site measurement and engineering experience, the three-dimensional stress of the coal pillar can be obtained, as σ_1=14.3 MPa, σ_2=11.2 MPa, σ_3=9.7 MPa.

Based on the Mohr-Coulomb strength criterion of Eq. (18), the triaxial strengths for rock mass of roof, floor and coal pillar are 102.65 MPa, 98.12 MPa and 34.07 MPa, respectively.

According to the Eqs. (22)-(25), the strengths of rock mass for roof and coal pillar in the interfacial area are 50.66 MPa and 142.07 MPa, respectively. And the strengths of rock mass for floor and coal pillar in the interfacial area are 47.56 MPa and 138.93 MPa, respectively. Therefore, the interfacial effect between the roof and coal pillar will decrease the strength of rock mass for roof very largely, and its strength is only about half of the original one. While the interfacial effect between the roof and coal pillar will increase the strength of coal pillar very largely, and its strength is about four times of the original one. And the same conclusion can be drawn for the interfacial area between the floor and coal pillar. Thus, the interfacial effect can improve the stability of the coal pillar very largely.

Moreover, for the interfacial effect, the strength of coal pillar will be larger than those of rock mass for roof and

Table 1 Mechanical parameters for coal pillar, roof and floor

Parameter	*E*/GPa	μ	*C*/MPa	φ/degrees	σ_c/MPa
Coal pillar	5.1	0.35	1.45	28	7.2
Roof	32	0.27	13.5	36	65.3
Floor	25	0.22	11.7	40	53.5

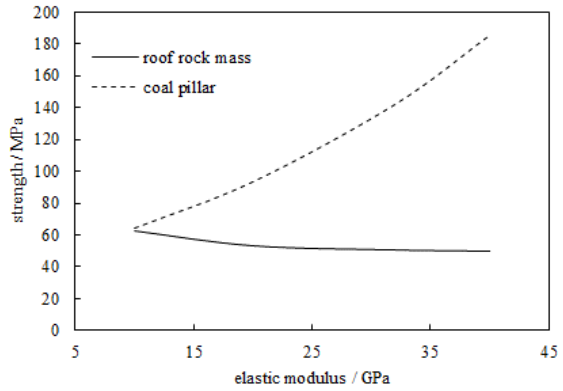

Fig. 4 Influence of the elastic modulus for rock mass of roof on the strength of roof and coal pillar

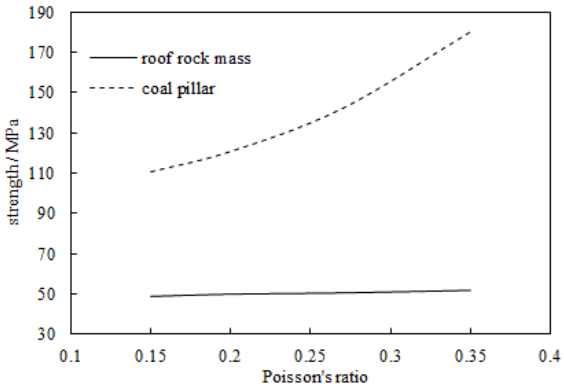

Fig. 5 Influence of the Poisson's ratio for rock mass of roof on the strength of roof and coal pillar

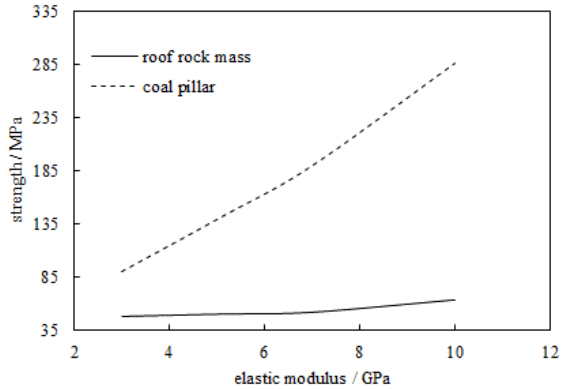

Fig. 6 Influence of the elastic modulus for coal pillar on the strength of roof and coal pillar

floor very much. Thus, the coal pillar will squeeze into the roof and floor, and cause the roof fall or floor heave, which can be found in previous studies (Gao 1998).

To analyze the influence of mechanical parameters of

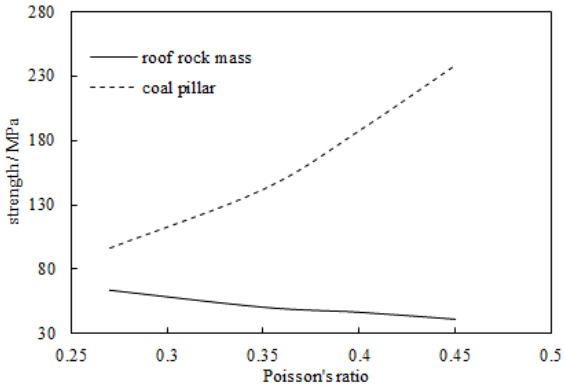

Fig. 7 Influence of the Poisson's ratio for coal pillar on the strength of roof and coal pillar

the elastic modulus and the Poisson's ratio on the interfacial effect, the interfacial area between roof and coal pillar is studied. However, the interfacial area between floor and coal pillar can be researched by the same method. In this study, only the mechanical parameters whose influence are researched are changed at the condition that the other parameters are fixed.

The influence of the elastic modulus of rock mass for roof on the strength of roof and coal pillar are shown in Fig. 4. The influence of the Poisson's ratio of rock mass for roof on the strength of roof and coal pillar are shown in Fig. 5.

As shown in Fig. 4, the strength of rock mass for roof and coal pillar are all affected by the elastic modulus of rock mass for roof. The relationship between the elastic modulus of roof and the strength of roof and coal pillar are all hyperbola. However, their changing laws are opposite. As the elastic modulus of roof increases, the strength of roof decreases, and the decreasing rate of the strength of roof decreases as well. On the contrary, as the elastic modulus of roof increases, the strength of coal pillar increases too, and the increasing rate of the strength of coal pillar increases as well. Moreover, the effect of the elastic modulus of roof on the strength of coal pillar is very serious, while the effect on the strength of roof is sometimes little. As shown in Fig. 5, the strength of roof and coal pillar are all affected by the Poisson's ratio of rock mass for roof too. The relationship between the Poisson's ratio of roof and the strength of roof is almost one straight line. As the Poisson's ratio of roof increases, the strength of roof increases too. However, the relationship between the Poisson's ratio of roof and the strength of coal pillar is hyperbola. As the Poisson's ratio of roof increases, the strength of coal pillar increases too, and the increasing rate of the strength of coal pillar increases as well. Moreover, the effect of the Poisson's ratio for roof on the strength of coal pillar is serious, while the effect on the strength of roof is very little. Compared Fig. 4 with Fig. 5, the follow conclusion can be drawn, the effect of elastic modulus is much larger than that of Poisson's ratio. And the effect on the strength of roof is much less than that on the strength of coal pillar.

Moreover, the influence of the elastic modulus for coal pillar on the strength of roof and coal pillar are shown in Fig. 6. The influence of the Poisson's ratio for coal pillar on

the strength of roof and coal pillar are shown in Fig. 7.

As shown in Fig. 6, the strength of roof and coal pillar are all affected by the elastic modulus of coal pillar. The relationship between the elastic modulus of coal pillar and the strength of roof is almost hyperbola. As the elastic modulus of coal pillar increases, the strength of roof increases too, and the increasing rate of the strength of roof increases as well. However, the relationship between the elastic modulus of coal pillar and the strength of coal pillar is almost one straight line. As the elastic modulus of coal pillar increases, the strength of coal pillar increases too. Moreover, the effect of the elastic modulus of coal pillar on the strength of coal pillar is very serious, while the effect on the strength of roof is very little. As shown in Fig. 7, the strength of roof and coal pillar are all affected by the Poisson's ratio of coal pillar. The relationship between the Poisson's ratio of coal pillar and the strength of roof and coal pillar are all hyperbola. However, their laws are opposite. As the Poisson's ratio of coal pillar increases, the strength of roof decreases, and the decreasing rate of the strength of roof decreases as well. On the contrary, as the Poisson's ratio of coal pillar increases, the strength of coal pillar increases too, and the increasing rate of the strength of coal pillar increases as well. Moreover, the effect of the Poisson's ratio of coal pillar on the strength of coal pillar is very serious, while the effect on the strength of roof is sometimes little. Compared Fig. 6 with Fig. 7, the follow conclusion can be drawn, the effect of elastic modulus is much larger than that of Poisson's ratio. And the effect on the strength of roof is much less than that on the strength of coal pillar.

7. Conclusions

Because the stress state of coal pillar is similar with that for rock specimen of the uniaxial compressive strength test, the constrained conditions of roof and floor for the coal pillar should affect the strength of coal pillar very seriously. To analyze the influence of rock mass for the roof and floor on the stability of coal pillar, one method was proposed. This method can obtain not only the derived stress by the cohesive constraining forces for the coal pillar, but also the derived stress for the rock mass of the roof and floor. Moreover, the effect of different mechanical parameters for the roof and floor on the stability of coal pillar have been analyzed more comprehensively. This method can not only analyze the stability of strip coal pillar, but also analyze the stability of other mining pillars whose stress distribution is similar with that of the strip coal pillar.

From the theoretical and the engineering application studies, the follow conclusions can be drawn.

• The interfacial effect between roof and coal pillar or floor and coal pillar can decrease the strength of rock mass for roof and floor very largely and increase the strength of coal pillar very largely. And the strength of coal pillar should be much larger than those of rock mass for roof and floor.

• As the elastic modulus of roof and floor increases, the strength of roof and floor decreases, and the strength of coal pillar increases. As the Poisson's ratio of roof and floor increases, the strength of roof and floor, and the strength of coal pillar all increases.

• As the elastic modulus of coal pillar increases, the strength of roof and floor, and the strength of coal pillar all increases. As the Poisson's ratio of coal pillar increases, the strength of roof and floor decreases, and the strength of coal pillar increases.

• The effect of elastic modulus is much larger than that of Poisson's ratio. And the effect on the strength of roof and floor is much less than that on the strength of coal pillar.

However, this is only one primary study, and the theoretical analysis only under certain assumptions for the influence of rock mass for the roof and floor on the stability of the coal pillar has been conducted. Moreover, the plastic failure of rock stratum is not considered. In-depth studies, such as field measurements, will be the subject of future work.

Acknowledgments

The Fundamental Research Fund for the Central Universities under Grant No. 2016B10214 is gratefully acknowledged.

References

Chen, M., Yang, S.Q., Zhang, Y.C. and Zang, C.W. (2016), "Analysis of the failure mechanism and support technology for the Dongtan deep coal roadway", *Geomech. Eng.*, **11**(3), 401-420.

Chen, S.J., Wang, H.L., Wang, H.Y., Guo, W.J. and Li, X.S. (2016), "Strip coal pillar design based on estimated surface subsidence in Eastern China", *Rock Mech. Rock Eng.*, **49**(9), 3829-3838.

Gao, W. (1998), "Study on the coal pillar stability of strip mining", M.Sc. Dissertation, China University of Mining and Technology, Xuzhou, China (in Chinese).

Gao, W. (2014), "Study on the width of the non-elastic zone in inclined coal pillar for strip mining", *J. Rock Mech. Min. Sci.*, **72**, 304-310.

Gao, W. and Ge, M.M. (2016), "Stability of a coal pillar for strip mining based on an elastic-plastic analysis", *J. Rock Mech. Min. Sci.*, **87**, 23-28.

Ghasemi, E., Ataei, M. and Shahriar, K. (2014), "Prediction of global stability in room and pillar coal mines", *Nat. Hazards*, **72**(2), 405-422.

Guo, W.B. and Cai, H.B. (2008), *Coal Mining Damage and Protection*, Coal Industry Press, Beijing, China (in Chinese).

Guo, W.J., Wang, H.L. and Chen, S.J. (2016), "Coal pillar safety and surface deformation characteristics of wide strip pillar mining in deep mine", *Arab. J. Geosci.*, **9**, 137.

Jaeger, C. (2009), *Rock Mechanics and Engineering*, Cambridge University Press, Cambridge, U.K.

Jia, S.C., Wang, J.C. and Zhu, J.M. (2011), "Calculation and application on elastic-plastic coal pillar width of the stope", *Proc. Eng.*, **26**, 1116-1124.

Jin, P.J., Wang, E.Y. and Song, D.Z. (2017), "Study on correlation of acoustic emission and plastic strain based on coal-rock damage theory", *Geomech. Eng.*, **12**(4), 627- 637.

Li, J.J. and Lian, M.J. (2011), *Rock Mechanics in Mining*, Metallurgical Industry Press, Beijing, China (in Chinese).

Li, Q., Xu, H., Bu, W.K. and Zhao, G.Z. (2011), "An analytic

solution describing the visco-elastic deformation of coal pillars in room and pillar mine", *Min. Sci. Tech. (China)*, **21**(6), 885-890.

Li, W.F., Bai, J.B., Peng, S., Wang, X.Y. and Xu, Y. (2015), "Numerical modeling for yield pillar design: A case study", *Rock Mech. Rock Eng.*, **48**(1), 305-318.

Mark, C. (1999), "The state-of-the-art in coal pillar design", *Proceeding of the 1999 SME Annual Meeting*, Denver, Colorado, U.S.A. March.

Reed, G., Mctyer, K. and Frith, R. (2017), "An assessment of coal pillar system stability criteria based on a mechanistic evaluation of the interaction between coal pillars and the overburden", *J. Min. Sci. Technol.*, **27**(1), 9-15.

Sadd, M.H. (2005), *Elasticity: Theory, Applications and Numerics*, Elsevier, Oxford, U.K.

Shao, X.P. and Xia, Y.C. (2011), "Modeling and numerical optimal simulation of coal pillar's failure process on longwall leaving coal pillar mining", *Appl. Mech. Mater.*, **88**, 285-290.

Sherizadeh, T. and Kulatilake P.H.S.W. (2016), "Assessment of roof stability in a room and pillar coal mine in the U.S. using three-dimensional distinct element method", *Tunn. Undergr. Sp. Technol.*, **59**, 24-37.

Tan, X.S. and Xian, X.F. (1994), *Theory of Composite Rock Mechanics and Its Applications*, Coal Industry Press, Beijing, China (in Chinese).

Wang, J., Jiang, J.Q., Li, G.B. and Hu, H. (2016), "Exploration and numerical analysis of failure characteristic of coal pillar under great mining height longwall influence", *Geotech. Geolog. Eng.*, **34**(2), 689-702.

Wattimena, R.K., Kramadibrata, S., Sidi, I.D. and Azizi, M.A. (2013), "Developing coal pillar stability chart using logistic regression", *J. Rock Mech. Min. Sci.*, **58**, 55-60.

Wilson, A.H. (1972), "An hypothesis concerning pillar stability", *Min. Eng.*, **131**, 409-417.

Wu, L.X., Wang, J.Z., Xing, A.S. and Liu, Y.A. (1994), *Strip Mining Theories and Its Applications under Buildings*, China University of Mining and Technology Press, Xuzhou, China (in Chinese).

Yang, J.X., Liu, Y., Yu, B. and Wu, F.F. (2015), "The effect of a multi-gob, pier-type roof structure on coal pillar load-bearing capacity and stress distribution", *Bull. Eng. Geol. Environ.*, **74**(4), 1267-1273.

Zhang, G.C., He, F.L., Jia, H.G. and Lai, Y.H. (2017), "Analysis of gateroad stability in relation to yield pillar size: A case study", *Rock Mech. Rock Eng.*, **50**(5), 1263-1278.

Zhang, H., Elsworth, D. and Wan, Z. (2018), "Failure response of composite rock-coal samples", *Geomech. Geophys. Geo-energ. Geo-resour.*, **4**(2), 175-192.

Zhang, J.X., Huang, P., Zhang, Q., Li, M. and Chen, Z.W. (2017), "Stability and control of room mining coal pillars-taking room mining coal pillars of solid backfill recovery as an example", *J. Cent. South Univ.*, **24**(5), 1121-1132.

Zhang, W.G. and Goh, A.T.C. (2016), "Predictive models of ultimate and serviceability performances for underground twin caverns", *Geomech. Eng.*, **10**(2), 175-188.

Zhang, Y., Wan, Z.J., Li, F.C., Zhou, C.B., Zhang, B., Guo, F. and Zhu, C.T. (2013), "Stability of coal pillar in gob-side entry driving under unstable overlying strata and its coupling support control technique", *J. Min. Sci. Tech.*, **23**(2), 193-199.

Zhao, T.B., Guo, W.Y., Lu, C.P. and Zhao, G.M. (2016), "Failure characteristics of combined coal-rock with different interfacial angles", *Geomech. Eng.*, **11**(3), 345-359.

Zhou, J., Li, X.B., Shi, X.Z., Wei, W. and Wu, B.B. (2011), "Predicting pillar stability for underground mine using Fisher discriminant analysis and SVM methods", *Trans. Nonferrous Met. Soc. China*, **21**(12), 2734-2743.

Zhou, Z., Chen, L., Cai, X., Shen, B.T., Zhou, J. and Du, K. (2018), "Experimental investigation of the progressive failure of multiple pillar-roof system", *Rock Mech. Rock Eng.*, **51**(5), 1629-1636.

Zhou, Z., Chen, L., Zhao, Y., Zhao, T.B., Cai, X. and Du, X.M. (2017), "Experimental and numerical investigation on the bearing and failure mechanism of multiple pillars under overburden", *Rock Mech. Rock Eng.*, **50**(4), 995-1010.

CC